Materials Physics and Mechanics 47 (2021) 937-950
Research article

Received: September 24, 2021
Accepted: December 12, 2021

# EFFECTIVE DIFFUSIVITY OF TRANSVERSELY ISOTROPIC MATERIAL WITH EMBEDDED PORES

**K.P. Frolova✉, E.N. Vilchevskaya**

Institute for Problems of Mechanical Engineering RAS, 61, Bolshoi Pr. V.O., St. Petersburg, Russian Federation, 199178

✉ kspfrolova@gmail.com

**Abstract.** The paper is concerned with the calculation of the effective diffusivity of transversely isotropic material with spheroidal pores by means of effective field methods. The segregation effect that is the main difference between conductivity and diffusivity problems is taken into account. Wiener's and Hashin-Shtrikman's bounds are modified to account for the segregation. Orientational scatter of pores about a preferential orientation is considered. Mori-Tanaka, Kanaun-Levin, and Maxwell homogenization schemes in terms of property contribution tensors are used. The calculated diffusion coefficients depend on the volume fraction, the shape of pores, their distribution over orientations in a three-dimensional solid, and the segregation factor.

**Keywords:** effective field methods, effective diffusivity, segregation effect, bounds for diffusivity

***Acknowledgements***. *Support of this work by grant No. 20-08-01100 from the Russian Foundation for Basic Research is gratefully acknowledged.*

**Citation:** Frolova K.P., Vilchevskaya E.N. Effective diffusivity of transversely isotropic material with embedded pores // Materials Physics and Mechanics. 2021, V. 47. N. 6. P. 937-950. DOI: 10.18149/MPM.4762021_12.

## 1. Introduction

The microstructure of the host material can affect significantly the mass transport process inside it. Grain boundaries in metals provide high diffusivity paths [1]; phases in composites are characterized by different diffusivity [2]; vacancies, voids, and microcracks are known to be traps for impurities [3-6]. Accurate measurement of diffusion coefficients of materials with a complex microstructure faces difficulties. Thus, theoretical estimation of the effective diffusivity of composites is of great importance. In particular, the study of materials with discontinuities is of practical interest.

Hart [7] suggested using the mixture rule to estimate the role of dislocations in bulk diffusion. On the basis of similarity between governing equations in the diffusivity and conductivity problems, Barrer [8] rewrote a number of micromechanical schemes accounting for the interactions between inhomogeneities to estimate the effective diffusivity of material. Zhang and Liu [9] noticed a principal difference between diffusivity and conductivity problems: temperature is a continuous function across the phase boundaries, while concentration is usually not. To account for the jump in concentration, the segregation factor equal to the ratio of the impurity concentration in the matrix to the impurity concentration inside the inhomogeneities can be introduced [10,11]. Belova and Murch [12,13] introduced

http://dx.doi.org/10.18149/MPM.4762021_12

the segregation factor in Hart and Maxwell–Garnett equations to calculate effective properties of material consisting of grain boundaries and spherical grains. Knyazeva et al. [14] rewrote non-interaction approximation, Mori-Tanaka effective field method, and Maxwell homogenization scheme in terms of contribution tensors and calculated the effective diffusion coefficient of isotropic material consisting of spheroidal grains representing inhomogeneities and grain boundaries representing the matrix. Note that in the absence of the segregation effect, the results obtained in [14] coincide with the ones obtained under consideration of the conductivity problem. The last one was solved by means of various micromechanical schemes in a number of works considering materials with ellipsoidal and, in particular, spheroidal inhomogeneities (see, for example, [15-17]).

The present paper generalizes the results obtained by Knyazeva et al. [14] for isotropic material to the case of transversely isotropic material. The overall anisotropy is assumed to be induced by the shape and preferential orientation of inhomogeneities, whereas the host matrix is assumed to be isotropic.

We should note that paper [14] did not account for the jump in concentration at the matrix/inhomogeneity interface at every step of modeling. This led to incorrect estimations of the effective diffusivity when concentration is not a continuous function. The present paper provides correct expressions for effective diffusivity. Additionally, in contrast to [14], where they considered the grain boundaries processing high diffusivity as the matrix, we consider pores with high diffusivity as embedded inhomogeneities. Transversely isotropic materials consisting of matrix and spheroidal pores can model layered metals with intergranular microcracks, which have a preferential orientation. For example, metals with defects created during formation or metals with hydrogen-induced microcracks along grain boundaries.

The paper investigates the influence of the segregation effect on the effective diffusion coefficients calculated by means of micromechanical methods accounting for interactions between inhomogeneities. Mori-Tanaka, Kanaun-Levin, and Maxwell homogenization methods are used. These methods belong to the class of effective field methods, which can be used to calculate the effective properties of the material in the case of its anisotropy induced by the shape and preferential orientation of inhomogeneities. We have already obtained the results on the basis of the Maxwell homogenization scheme in [18], whereas the results obtained within the two other effective field methods are presented the first time.

Results obtained within various homogenization schemes must be in agreement with Wiener's and Hashin-Shtrikman's bounds. Within the frame of the present paper, we purpose a modification of these bounds to account for the segregation effect. Additionally, we discuss the mathematical restriction on the application of the Maxwell scheme due to singularity at a certain volume fraction of inhomogeneities. To avoid this non-physical effect in the elasticity problem, linearization of the Maxwell scheme with respect to interaction effect was proposed in [19]. Following [19], we propose a linearization of the Maxwell scheme for diffusivity.

## 2. Property contribution tensors

One can express the effect of a given inhomogeneity on the properties of interest in terms of property contribution tensors [20,21]. Sums of the property contribution tensors are proper microstructural parameters that reflect contributions of individual inhomogeneities to the overall properties. We focus on the influence of an isolated inhomogeneity on the diffusion process and introduce the second-rank diffusivity contribution tensor, $\mathbf{H}^{D}$, and resistance contribution tensor, $\mathbf{H}^{DR}$.

We start with consideration a reference volume $V$ of an infinite three-dimensional solid with the isotropic diffusivity tensor $\mathbf{D}_0=D_0\mathbf{I}$ containing inhomogeneity of volume $V_1<<V$ with the isotropic diffusivity tensor $\mathbf{D}_1=D_1\mathbf{I}$. The main difference between conductivity and diffusivity problems is a segregation effect specific to the last problem. To account for this

effect it is necessary to consider a discontinuous concentration field (a specific case of non-ideal contacts at the matrix/inhomogeneity interface). Following [13,22], the boundary conditions at the matrix (denoted by "+")/inhomogeneity (denoted by "-") interface are taken as

$$D_0 \frac{\partial c(x)}{\partial n}\Big|_{x\to\partial V1+} = D_1 \frac{\partial c(x)}{\partial n}\Big|_{x\to\partial V1-}, \quad (1)$$

$$c(x)|_{x\to\partial V1+} = sc(x)|_{x\to\partial V1-}, \quad (2)$$

where $c$ is concentration, $s$ is the segregation factor. The last one describes a constant jump in impurity concentration.

When there is no segregation effect, $s = 1$. In the cases when impurity can be partially trapped at the interface or inside inhomogeneities, $s > 1$ or $s < 1$, respectively. Grain boundaries, microcracks, pores, and other discontinuities are known to be traps for diffusing particles. Hence, a correct choice of the value of the segregation factor depends on the micromechanical model of a composite material, namely, which phase represents matrix, and which phase represents inhomogeneities. Knyazeva et al. [14] modeled grain boundaries through the matrix, and grains were considered as inhomogeneities. In this case, impurity is trapped in the matrix, so the authors considered s > 1. If grain boundaries represent inhomogeneities, impurity is trapped inside it, and s < 1. Similarly, when pores are introduced as embedded inhomogeneities, s < 1. Hereafter we focus on cases $s \le 1$.

If the concentration is prescribed on the boundary $\partial V$ ($c(x)|_{\partial V} = \mathbf{G}^0 \cdot \boldsymbol{x}$), whatever the composition and microstructure of the reference volume, the volume average of the concentration gradient at the absence of body sources is completely determined by its boundary values

$$\langle \nabla c \rangle_V = \frac{1}{V}\int_{\partial V} \mathbf{n}_V c_0 \, \mathrm{d}\partial V = \mathbf{G}^0, \quad (3)$$

where $\mathbf{n}_V$ is the outer unit normal vector on $\partial V$. Introducing the inner boundary $\partial V_1$ and taking into account that concentration is a discontinuous function, an application of the Gauss theorem yields

$$\langle \nabla c \rangle_V = \left(1 - \frac{V_1}{V}\right)\langle \nabla c \rangle_{V_0} + \frac{V_1}{V}\langle \nabla c \rangle_{V_1} + \frac{1}{V}\int_{\partial V_1} \mathbf{n}(c_0 - c_1)\mathrm{d}\partial V_1, \quad (4)$$

where $\langle\cdot\rangle_{V_0} = \int_{V_0} \cdot \, \mathrm{d}V_0$, $\langle\cdot\rangle_{V_1} = \int_{V_1} \cdot \, \mathrm{d}V_1$ denote spatial averaging over the matrix and inhomogeneity, respectively; $\mathbf{n}$ is the unit normal vector on the interface surface, pointing from the inhomogeneity to the matrix. The last term vanishes in the case of ideal contact. Note that paper [14] did not introduce the last term even in the case of non-ideal contact.

Taking into account the boundary condition (2), equation (4) results in

$$\langle \nabla c \rangle_V = \left(1 - \frac{V_1}{V}\right)\langle \nabla c \rangle_{V_0} + \mathrm{s}\frac{V_1}{V}\langle \nabla c \rangle_{V_1}. \quad (5)$$

The average concentration gradient can be alternatively found through the spatial averaging

$$\langle \nabla c \rangle_V = \frac{1}{V}\int_V \nabla c \, \mathrm{d}V = \frac{1}{V}\int_{V_0} \nabla c \, \mathrm{d}V_0 + \frac{1}{V}\int_{V_1} \nabla c \, \mathrm{d}V_1. \quad (6)$$

An application of the Gauss theorem, consideration of the boundary condition $c(x)|_{\partial V} = \mathbf{G}^0 \cdot \boldsymbol{x}$ and accounting for the presence of the inner boundary yields

$$\mathbf{G}^0 = \left(1 - \frac{V_1}{V}\right)\langle \nabla c \rangle_{V_0} + \mathrm{s}\frac{V_1}{V}\langle \nabla c \rangle_{V_1} \quad (7)$$

that coincides with equality (5).

The molar flux averaged over a reference volume depends on the microstructure of the material. It is a continuous function across the matrix/inhomogeneity interface, so

$$\langle \mathbf{J} \rangle_V = \left(1 - \frac{V_1}{V}\right)\langle \mathbf{J} \rangle_{V_0} + \frac{V_1}{V}\langle \mathbf{J} \rangle_{V_1}. \quad (8)$$

Assuming inhomogeneity and the surrounding material to satisfy the linear Fick's law, we obtain

$$\langle \mathbf{J} \rangle_V = -\left(1 - \frac{V_1}{V}\right) \mathbf{D}_0 \cdot \langle \nabla c \rangle_{V_0} - \frac{V_1}{V} \mathbf{D}_1 \cdot \langle \nabla c \rangle_{V_1} = -\mathbf{D}_0 \cdot \mathbf{G}^0 - \frac{V_1}{V} (\mathbf{D}_1 - s\mathbf{D}_0) \cdot \langle \nabla c \rangle_{V_1}. \quad (9)$$

Introducing the concentration tensor $\mathbf{\Lambda}_c$ that expresses the concentration gradient averaged over inhomogeneity in terms of $\mathbf{G}^0$ as $\langle \nabla c \rangle_{V_1} = \mathbf{\Lambda}_c \cdot \mathbf{G}^0$, formula (9) reduces to

$$\langle \mathbf{J} \rangle_V = -\left[\mathbf{D}_0 + \frac{V_1}{V} (\mathbf{D}_1 - s\mathbf{D}_0) \cdot \mathbf{\Lambda}_c\right] \cdot \mathbf{G}^0 = -\left[\mathbf{D}_0 + \frac{V_1}{V} \mathbf{H}^D\right] \cdot \mathbf{G}^0. \quad (10)$$

The second term in the brackets represents the contribution of the inhomogeneity into overall diffusivity.

In the case when the molar flux $\mathbf{J}^0$ is prescribed at the boundary of $V$ instead of the concentration, $\langle \mathbf{J} \rangle_V = \mathbf{J}^0$, and the concentration gradient depends on the microstructure of the material. Hence,

$$\langle \nabla c \rangle_V = -\boldsymbol{D}_0^{-1} \cdot \mathbf{J}^0 - \frac{V_1}{V} (s\boldsymbol{D}_1^{-1} - \boldsymbol{D}_0^{-1}) \cdot \langle \mathbf{J} \rangle_{V_1}. \quad (11)$$

Introducing tensor $\mathbf{\Lambda}_j$ that expresses the molar flux averaged over inhomogeneity in terms of $\mathbf{J}^0$ as $\langle \mathbf{J} \rangle_{V_1} = \mathbf{\Lambda}_j \cdot \mathbf{J}^0$, formula (11) reduces to

$$\langle \nabla c \rangle_V = -\left[\boldsymbol{D}_0^{-1} + \frac{V_1}{V} (s\boldsymbol{D}_1^{-1} - \boldsymbol{D}_0^{-1}) \cdot \mathbf{\Lambda}_j\right] \cdot \mathbf{J}^0 = -\left[\boldsymbol{D}_0^{-1} + \frac{V_1}{V} \mathbf{H}^{DR}\right] \cdot \mathbf{J}^0. \quad (12)$$

Tensors $\mathbf{\Lambda}_j$ and $\mathbf{\Lambda}_c$ are related as $\mathbf{\Lambda}_j = \mathbf{D}_1 \cdot \mathbf{\Lambda}_c \cdot \boldsymbol{D}_0^{-1}$, so we finally obtain $\mathbf{H}^{DR} = -(1/D_0^2)\mathbf{H}^D$.

Explicit analytical expressions for the concentration tensor can be obtained in the case of ellipsoidal inhomogeneity only. Following Fricke [23] for electrical conductivity (where the potential is a continuous function across the matrix/inhomogeneity interface) and using boundary conditions (1)-(2) instead of the ones considered in [23], the expression for the concentration tensor of spheroidal inhomogeneity with the symmetry axis along a unit vector $\mathbf{n}$ takes the form [14]

$$\mathbf{\Lambda}_c = \frac{D_0}{sD_0 + (D_1 - sD_0) f_0} \boldsymbol{\theta} + \frac{D_0}{D_1 - 2(D_1 - sD_0) f_0} \mathbf{nn}, \quad (13)$$

where $\boldsymbol{\theta} = \mathbf{I} - \mathbf{nn}$. The shape function $f_0$ depends on the aspect ratio of the spheroidal inhomogeneity $\gamma$ ($\gamma < 1$, $\gamma = 1$, and $\gamma > 1$ correspond respectively to an oblate spheroid, sphere, and prolate spheroid) in the following way

$$f_0(\gamma) = \frac{1 - g}{2(1 - \gamma^{-2})},$$

where

$$g(\gamma) = \begin{cases} \dfrac{1}{\gamma\sqrt{1 - \gamma^2}} \arctan \dfrac{\sqrt{1 - \gamma^2}}{\gamma}, \gamma \le 1 \\ \dfrac{1}{2\gamma\sqrt{\gamma^2 - 1}} \ln\left(\dfrac{\gamma + \sqrt{\gamma^2 - 1}}{\gamma - \sqrt{\gamma^2 - 1}}\right), \gamma \ge 1. \end{cases}$$

The diffusivity contribution tensors take the form

$$\mathbf{H}^D = -D_0^2 \mathbf{H}^{DR} = D_0 [B_1 \boldsymbol{\theta} + B_2 \mathbf{nn}], \quad (14)$$

where introducing $\alpha = D_0 / D_1$,

$$B_1 = \frac{1 - s\alpha}{s\alpha + (1 - s\alpha) f_0}, B_2 = \frac{1 - s\alpha}{1 - 2(1 - s\alpha) f_0}.$$

Note that coefficients $B_1$ and $B_2$ and, therefore, the contribution tensors, do not depend on the segregation factor at $\alpha = 0$ (that corresponds to $D_1 \to \infty$).

The concentration tensor can be alternatively written in terms of first Hill's tensor $\mathbf{P} = \left(\nabla \int_{V_1} \nabla' G(x - x') dx'\right)^S$ ($G$ is the Green's function for concentration). Hill's tensor for spheroidal inhomogeneity is as follows [20]

$$\mathbf{P} = \frac{1}{D_0} [f_0 \boldsymbol{\theta} + (1 - 2f_0) \mathbf{nn}]. \quad (15)$$

To account for a jump in concentration at the matrix/inhomogeneity interface, a double layer potential must be introduced in a classical approach that considers inhomogeneity with ideal contacts. The result is as follows

$$\mathbf{\Lambda}_c = [\mathrm{s}\mathbf{I} + (\mathbf{D}_1 - \mathrm{s}\mathbf{D}_0) \cdot \mathbf{P}]^{-1}. \tag{16}$$

Then, the diffusivity contribution tensor can be expressed in terms of $\mathbf{P}$ as

$$\mathbf{H}^D = \left[\left(\frac{1}{s}\mathbf{D}_1 - \mathbf{D}_0\right)^{-1} + \mathbf{P}\right]^{-1}, \tag{17}$$

and resistance contribution tensor can be expressed in terms of second Hill's tensor $\mathbf{Q} = \mathbf{D}_0 \cdot (\mathbf{I} - \mathbf{P} \cdot \mathbf{D}_0)$ as

$$\mathbf{H}^{DR} = \left[\left(\left(\frac{1}{s}\mathbf{D}_1\right)^{-1} - \boldsymbol{D}_0^{-1}\right)^{-1} + \mathbf{Q}\right]^{-1}. \tag{18}$$

It is seen that the obtained contribution tensors coincide with the contribution tensors used in the problem with ideal contacts if $\widetilde{D}_1 = D_1/s$ being diffusivity of inhomogeneity. Thus, inhomogeneity with non-ideal contacts can be replaced by the "effective inhomogeneity" with ideal contacts.

## 3. Homogenization methods

Effective properties of the material with multiple inhomogeneities can be calculated using approximate homogenization methods. A detailed historical review of micromechanical methods can be found in [24], whereas the current state of knowledge of the problem is described in [20].

The class of effective field methods simulates the effect of interaction between isolated inhomogeneities by placing them in a certain effective field that generally differs from the applied one [25]. The scheme, proposed by Mori and Tanaka [26] and clarified by Benveniste [27], assumes that each inhomogeneity is placed into a uniform field that is equal to its average over the matrix. Following [20] for conductivity, we rewrite the Mori-Tanaka scheme in terms of property contribution tensors. The effective diffusivity accounting for the segregation effect then takes the form

$$\mathbf{D}^{\mathrm{eff}} = \mathbf{D}_0 + \frac{1}{V}\sum_i V_i \mathbf{H}_i^D \cdot \left[\left(\frac{1}{s}\mathbf{D}_1 - \mathbf{D}_0\right)^{-1} \cdot \frac{1}{V}\sum_i V_i \mathbf{H}_i^D + (1-\phi)\mathbf{I}\right]^{-1} = \left\{\mathbf{D}_0^{-1} + \frac{1}{V}\sum_i V_i \mathbf{H}_i^{DR} \cdot \left[\left(\left(\frac{1}{s}\mathbf{D}_1\right)^{-1} - \boldsymbol{D}_0^{-1}\right)^{-1} \cdot \frac{1}{V}\sum_i V_i \mathbf{H}_i^{DR} + (1-\phi)\mathbf{I}\right]^{-1}\right\}^{-1}, \tag{19}$$

where $\phi$ is the volume fraction of inhomogeneities, and contribution tensors are defined by equations (14).

Maxwell scheme can be considered as a version of the effective field method [20]. According to Maxwell's idea [28], calculation of the effective properties is based on the evaluation of far-field perturbations due to inhomogeneities in two different ways and subsequent equation the results. The first way is to evaluate this field as the one generated by some homogenized region that can be considered as an effective inhomogeneity possessing (yet) unknown effective properties. The second way is based on consideration of the sum of far fields generated by all the individual inhomogeneities within this domain (treated as non-interacting ones). Maxwell's scheme for elasticity and conductivity problems was rewritten in terms of property contribution tensors in [29,30,31]. In a similar way, for diffusivity the equating of two results yields

$$\frac{\mathrm{V}^*}{V}\mathbf{H}_{\mathrm{eff}}^D = \frac{1}{V}\sum_i V_i \mathbf{H}_i^D \quad \text{or} \quad \frac{\mathrm{V}^*}{V}\mathbf{H}_{\mathrm{eff}}^{DR} = \frac{1}{V}\sum_i V_i \mathbf{H}_i^{DR}, \tag{20}$$

where $\mathbf{H}_{\mathrm{eff}}^D, \mathbf{H}_{\mathrm{eff}}^{DR}$ are contribution tensors of the effective inhomogeneity denoted by *. The contribution tensors depend on the shape of the effective inhomogeneity. Explicit analytical

expressions for $\mathbf{H}_{\text{eff}}^{D}, \mathbf{H}_{\text{eff}}^{DR}$ are available for the ellipsoidal shapes only, and in this case, equation (20) can be explicitly solved. Recommendations regarding the choice of the shape of the effective inhomogeneity are given in [29]. In the case of transversely isotropic microstructure, the domain is spheroidal with the aspect ratio

$$\gamma^* = \frac{\frac{1}{V}\sum_i V_i P_{11}}{\frac{1}{V}\sum_i V_i P_{33}}. \tag{21}$$

Assuming a constant jump in concentration at the matrix/effective inhomogeneity interface defined by the segregation factor $s^*$, we deal with $\mathbf{H}_{\text{eff}}^{D} = \mathbf{H}_{\text{eff}}^{D}(s^*, \dots), \mathbf{H}_{\text{eff}}^{DR} = \mathbf{H}_{\text{eff}}^{DR}(s^*, \dots)$. In this case, expression of the left-hand sides in equations (20) by formulas (17), (18) taking $= s^*$, $\mathbf{D}_1 = \mathbf{D}^{\text{eff}}$, and $\mathbf{P} = \mathbf{P}^*, \mathbf{Q} = \mathbf{Q}^*$ results in

$$\mathbf{D}^{\text{eff}} = s^* \left\{ \mathbf{D}_0 + \left[ \left( \frac{1}{V}\sum_i V_i \mathbf{H}_i^{D} \right)^{-1} - \mathbf{P}^* \right]^{-1} \right\} = s^* \left\{ \mathbf{D}_0^{-1} + \left[ \left( \frac{1}{V}\sum_i V_i \mathbf{H}_i^{DR} \right)^{-1} - \mathbf{Q}^* \right]^{-1} \right\}^{-1}. \tag{22}$$

Formula (22) can be alternatively obtained by considering of effective homogenized region with $\mathbf{D}_*^{\text{eff}} = \mathbf{D}^{\text{eff}}/s^*$ in a Maxwell scheme written for material with ideal contacts at the matrix/effective inhomogeneity interface.

According to formulas (22), effective properties are strongly dependent on the segregation factor $s^*$ that defines a jump in concentration on a fictive boundary $\partial V^*$ and can not be measured. In particular, when $s^* = 0$, the composite material becomes impenetrable. This seems to be non-reasonable, so hereafter we take $s^* = 1$.

Kanaun-Levin effective field method [32,33] places each inhomogeneity into a certain effective field dependent on the spatial statistics of inhomogeneities' centers. The statistical information is described in terms of characteristic functions of the domains occupied by inhomogeneities. Each inhomogeneity is surrounded by a certain prohibition zone, which neighbor inhomogeneities cannot enter. The prohibition zone is assumed to have an ellipsoidal shape described by some tensor $\boldsymbol{\alpha}$.

Following [20], where the Kanaun-Levin method was rewritten in the context of conductivity in terms of property contribution tensors, we can obtain the following expressions for the problem in the context of diffusivity:

$$\mathbf{D}^{\text{eff}} = \mathbf{D}_0 + \left[ \left( \frac{1}{V}\sum_i V_i \mathbf{H}_i^{D} \right)^{-1} - \mathbf{P}(\boldsymbol{\alpha}) \right]^{-1}, \tag{23}$$

where tensor $\mathbf{P}(\boldsymbol{\alpha})$ is the Hill's tensor reflecting the shape of the ellipsoidal prohibition zone.

When the prohibition zone is spheroidal, $\mathbf{P}(\boldsymbol{\alpha})$ is given by equation (15) at $\gamma = \gamma^{\boldsymbol{\alpha}}$ being the aspect ratio of the spheroidal prohibition zone and $\mathbf{n}$ being a unit vector along its symmetry axis. Within the frame of the present paper, we consider three shapes of the prohibition zone in Kanaun-Levin scheme, namely,

1. Shape of the prohibition zone coincides with the shape of an individual inhomogeneity;
2. Shape of the prohibition zone is spherical (the case of random distribution of inhomogeneities' centers);
3. Shape of the prohibition zone coincides with the shape of some effective inhomogeneity. This shape can be determined similarly to the homogenization area in the Maxwell scheme. In this case, Kanaun-Levin scheme gives the same results as the Maxwell scheme.

According to formulas (19), (22), (23), the effective diffusivity can be alternatively calculated by replacing inhomogeneities with non-ideal contacts by effective inhomogeneities with ideal contacts characterized by $\widetilde{D}_1 = D_1/s$. The results obtained within the three effective field methods coincide at the same conditions as in the conductivity problem (the last one are listed in [20]).

Note that the Mori-Tanaka scheme gives a physically consistent result at any value of the volume fraction of inhomogeneities. In particular, at $\phi$ = 1 this scheme results in $\mathbf{D}^{\text{eff}} = \widetilde{\mathbf{D}}_1$ that means that the properties of composite material are fully determined by properties of inhomogeneity. If $\widetilde{\mathbf{D}}_1 = \mathbf{D}_1/s$, the overall diffusivity depends on the segregation factor. Maxwell and Kanaun-Levin's homogenization methods give appropriate results at $\phi$ = 1 only in the case of parallel spheroids when the prohibition zone coincides with the shape of individual inhomogeneity.

In addition, in the general case of distribution of inhomogeneities over orientations, there is a mathematical restriction on the use of Maxwell and Kanaun-Levin homogenization schemes, namely, expressions in the square brackets in equations (22) and (23) must not be equal to zero (if they equal to zero, the second terms go to infinity due to inversion).

To avoid the artificial effect due to singularity that does not have a physical meaning, linearization of the Maxwell scheme with respect to the interaction effect can be done. Following [19], where the linearization was proposed for the elasticity problem, we can rewrite equation (22) in the form

$$\mathbf{D}^{\text{eff}} = \mathbf{D}_0 + \frac{1}{V}\sum_i V_i \mathbf{H}_i^D \cdot \left[\mathbf{I} - \mathbf{P}^* \cdot \frac{1}{V}\sum_i V_i \mathbf{H}_i^D\right]^{-1} \tag{24}$$

that may be linearized as

$$\mathbf{D}^{\text{eff}} \approx \mathbf{D}_0 + \frac{1}{V}\sum_i V_i \mathbf{H}_i^D + \frac{1}{V}\sum_i V_i \mathbf{H}_i^D \cdot \mathbf{P}^* \cdot \frac{1}{V}\sum_i V_i \mathbf{H}_i^D. \tag{25}$$

Note that here we calculate the effective diffusivity in terms of diffusivity contribution tensor to avoid singularity occurring if we use resistance contribution tensors.

The effective diffusivity calculated using homogenization schemes must be in agreement with Wiener's bounds (analogs of the Voigt–Reuss bounds in elasticity) and Hashin–Shtrikman's bounds. Violation of the bounds constitutes a serious drawback. Following [20] for conductivity and introducing the diffusion coefficient of inhomogeneity with ideal contacts $\widetilde{D}_1 \geq D_0$, we rewrite the Wiener's bounds as

$$\frac{D_0 \widetilde{D}_1}{D_0\phi + \widetilde{D}_1(1-\phi)} \leq \mathrm{D}^{\text{eff}} \leq D_0(1-\phi) + \widetilde{D}_1\phi, \tag{26}$$

and Hashin–Shtrikman's bounds as

$$D_0 + \frac{\phi}{\frac{(1-\phi)}{3D_0} + \frac{1}{\widetilde{D}_1 - D_0}} \leq \mathrm{D}^{\text{eff}} \leq \widetilde{D}_1 + \frac{1-\phi}{\frac{\phi}{3\widetilde{D}_1} + \frac{1}{D_0 - \widetilde{D}_1}}. \tag{27}$$

Assuming $\widetilde{D}_1 = D_1/s$ and $\alpha = D_0/D_1$, restrictions (26) result in

$$\frac{1}{\alpha\phi s + (1-\phi)} \leq \frac{\mathrm{D}^{\text{eff}}}{D_0} \leq (1-\phi) + \phi\frac{1}{s\alpha} \tag{28}$$

and Hashin–Shtrikman's bounds (27) yield

$$1 + \frac{3\phi(1-s\alpha)}{(1-\phi)(1-s\alpha)+3s\alpha} \leq \frac{\mathrm{D}^{\text{eff}}}{D_0} \leq \frac{1}{\alpha s} + \frac{1}{\alpha s}\frac{3(1-\phi)(\alpha s-1)}{\phi(\alpha s-1)+3} \tag{29}$$

The Hashin-Shtrikman's bounds are more accurate than Wiener's ones. When $\alpha = 0$ ($D_1 \to \infty$), restrictions (28), (29) reduce respectively to

$$\frac{1}{1-\phi} \leq \frac{\mathrm{D}^{\text{eff}}}{D_0} < \infty, \quad \frac{1+2\phi}{1-\phi} \leq \frac{\mathrm{D}^{\text{eff}}}{D_0} < \infty.$$

As in conductivity, results obtained within the frame of Maxwell scheme coincide with Hashin–Shtrikman's lower bound in the case of spherical inhomogeneities.

**Effective properties of transversely isotropic material.** The summation over identical inhomogeneities can be replaced by multiplication of the volume fraction by tensors averaged over orientations (denoted by < >). Within the frame of the present research, we consider transversely isotropic material, so taking $\mathbf{m}$ to be the unit vector along the symmetry axis, the averaged contribution tensors can be rewritten in the following way:

$$\langle \mathbf{H}^D \rangle = D_0[a\boldsymbol{\theta} + b\mathbf{mm}]. \tag{30}$$

The coefficients $a$ and $b$ depend on the distribution of inhomogeneities over orientations. In the present research, we account for orientational scatter of pores about a preferential orientation that is described by means of the probability density function defined on the upper semisphere of unit radius ($0 \le \theta \le \pi/2$) [29]:

$$\psi_\lambda(\theta) = \frac{1}{2\pi}\left[(\lambda^2+1)e^{-\lambda\theta} + \lambda e^{-\lambda\pi/2}\right]. \quad (31)$$

The scatter parameter $\lambda$ varies in the range from zero to infinity that corresponds to fully random and strictly parallel orientations of inhomogeneities, respectively.

According to formulas (14), averaging of the property contribution tensors is equivalent to averaging of dyads **nn**. As a result,

$$a = B_1(1-g_1) + B_2 g_1, b = B_1(1-g_2) + B_2 g_2, \quad (32)$$

where $g_1$ and $g_2$ are functions of the scatter parameter:

$$g_1(\lambda) = \frac{18 - e^{-\frac{\lambda\pi}{2}}\lambda(3+\lambda^2)}{6(9+\lambda^2)},\ g_2(\lambda) = \frac{\left(3+e^{-\frac{\lambda\pi}{2}}\lambda\right)(3+\lambda^2)}{3(9+\lambda^2)}.$$

In the limit case of fully random orientations of pores,

$$a = b = \frac{2B_1}{3} + \frac{B_2}{3} = \eta(s,\gamma,\alpha), \quad (33)$$

whereas in the case of perfectly parallel orientation distribution of pores,

$$a = B_1(s,\gamma,\alpha), b = B_2(s,\gamma,\alpha). \quad (34)$$

Hence, taking $\mathbf{m} = \mathbf{e}_3$ equation (19) obtained within the frame of Mori-Tanaka effective field method reduces to

$$\mathbf{D}^{\text{eff}} = D_0\left(1 + \frac{\phi(1-s\alpha)a}{\phi a s\alpha + (1-\phi)(1-s\alpha)}\right)\boldsymbol{\theta} + D_0\left(1 + \frac{\phi(1-s\alpha)b}{\phi b s\alpha + (1-\phi)(1-s\alpha)}\right)\mathbf{mm}, \quad (35)$$

equation (22) obtained by means of Maxwell scheme can be rewritten as

$$\mathbf{D}^{\text{eff}} = D_0\left(1 + \frac{\phi a}{1-\phi a D_0 P_{11}^*}\right)\boldsymbol{\theta} + D_0\left(1 + \frac{\phi b}{1-\phi b D_0 P_{33}^*}\right)\mathbf{mm}, \quad (36)$$

and equation (23) obtained on the base of the Kanaun-Levin scheme takes the form

$$\mathbf{D}^{\text{eff}} = D_0\left(1 + \frac{\phi a}{1-\phi a D_0 P_{11}(\boldsymbol{\alpha})}\right)\boldsymbol{\theta} + D_0\left(1 + \frac{\phi b}{1-\phi b D_0 P_{33}(\boldsymbol{\alpha})}\right)\mathbf{mm}. \quad (37)$$

The mathematical restrictions due to singularity according to equations (36), (37) are as follows

$$\begin{cases} \phi < \frac{1}{a(s,\gamma,\alpha)D_0 P_{11}(D_0,\hat{\gamma})}, \\ \phi < \frac{1}{b(s,\gamma,\alpha)D_0 P_{33}(D_0,\hat{\gamma})}, \end{cases} \quad (38)$$

where, $\hat{\gamma} = \gamma^{\boldsymbol{\alpha}}$ in the case of the Kanaun-Levin scheme and, $\hat{\gamma} = \gamma^*$ in the case of Maxwell scheme.

According to restrictions (38), the limit value of the volume fraction of strictly parallel inhomogeneities is equal or greater than one (that can be considered as a "physical limit"). In the cases of non-parallel orientation distribution, this limit value can be less than one. In particular, in the case of random distribution of pores over orientations,

$$\phi < \frac{3}{\eta(s,\gamma,\alpha)}.$$

The linearized Maxwell scheme (25) results in

$$\mathbf{D}^{\text{eff}} \approx D_0\{(1 + \phi a(s,\gamma,\alpha) + \phi^2 a^2(s,\gamma,\alpha)D_0 P_{11}^*)\boldsymbol{\theta} + (1 + \phi b(s,\gamma,\alpha) + \phi^2 b^2(s,\gamma,\alpha)D_0 P_{33}^*)\mathbf{mm}\}. \quad (39)$$

## 4. Results and Discussion

To be specific, we consider the material with the ratio of the diffusion coefficient of background matrix consisting of grains and grain boundaries to the diffusion coefficient of pores $\alpha$ = 0.05 (see [18] for details). The shape of the oblate spheroidal pores is characterized

by $\gamma = 0.1$, whereas the shape of prolate spheroidal pores is characterized by $\gamma = 10$ (in the case of spherical pores, $\gamma = 1$).

Let us first check whether the results obtained by classical and linearized Maxwell scheme, Mori-Tanaka (M-T), and Kanaun-Levin (K-L) effective field methods are in agreement with the Wiener's and Hashin-Shtrikman's (H-S) bounds in the case of non-unit segregation factor. To be specific, we consider $s = 0.5$ and restrict ourselves to the investigation of the material with random orientation distribution of pores. We additionally assume a random distribution of inhomogeneities' centers to deal with isotropic material. In this case, $\gamma^{\alpha} = \gamma^{*} = 1$, so the Kanaun-Levin scheme coincides with the Maxwell scheme. The results are presented in Fig. 1. As it has been already mentioned, Hashin-Shtrikman's bounds are narrower than Wiener's bounds, and the last ones are not shown for the sake of brevity.

Figure 1(a) confirms that the Maxwell scheme, Kanaun-Levin scheme, and Mori-Tanaka scheme coincide with the Hashin-Shtrikman lower bound in the case of spherical pores. In the cases of oblate and prolate spheroidal pores, Maxwell and Kanaun-Lavin's schemes violate the upper bound due to non-physical singularity. The linearized Maxwell scheme does not have such a problem; however, it violates the lower bound at some value of the volume fraction of pores. At the same time, this value is greater than the value at which singularity takes place.

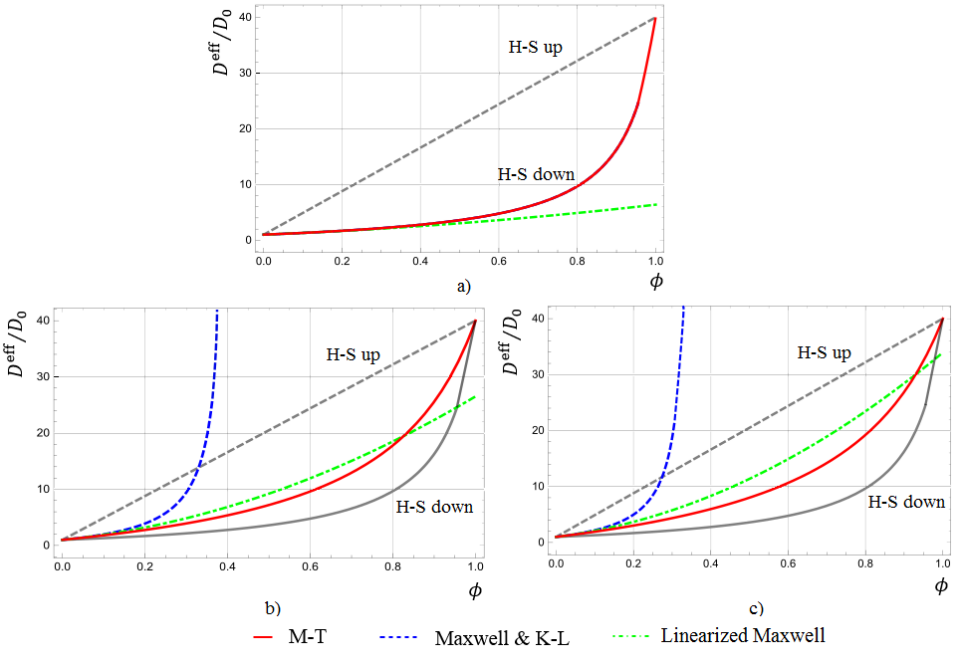


**Fig. 1.** Agreement of the homogenization schemes with H-S bounds in the cases of material with spherical pores (a), randomly oriented oblate pores (b), and randomly oriented prolate pores (c); $s = 0.5$

We now compare the results obtained by the Mori-Tanaka and Kanaun-Levin effective field method, and the Maxwell homogenization scheme in the context of the segregation effect. The accuracy of the Kanaun-Levin and Maxwell scheme is determined by the volume fraction of pores, so we compare the results at $\phi = 0.1$ because this value can be used when considering oblate, prolate and spherical pores. In this case, there is no need to consider the linearized Maxwell scheme, since it coincides with the general one at a low volume fraction of inhomogeneities.

Figure 2 shows the dependences of the normalized effective diffusion coefficient of the isotropic material on the segregation factor. Increasing a constant jump in concentration (i.e. decreasing the segregation factor) increases the effective diffusion coefficient and, therefore, mass permeability of the host material. From this point of view, segregation of particles inside pores produces an effect similar to increasing diffusivity of an inhomogeneity. This means that under a continuous flux more impurity enters the material (note that segregation in the model does not explain trapping, and the impurity is distributed uniformly across the reference volume). At the same time, segregation of impurity inside spherical pores does not increase the effective diffusion coefficient significantly. From this point of view, segregation inside pores increases the effect of the shape of the inhomogeneities on the overall diffusion coefficient. Hereafter we consider only oblate and prolate spheroidal pores. Decreasing the segregation factor increases the difference between the results obtained on the basis of various schemes. The segregation is seen to have a greater influence on the results obtained within the Maxwell and Kanaun-Levin homogenization schemes.

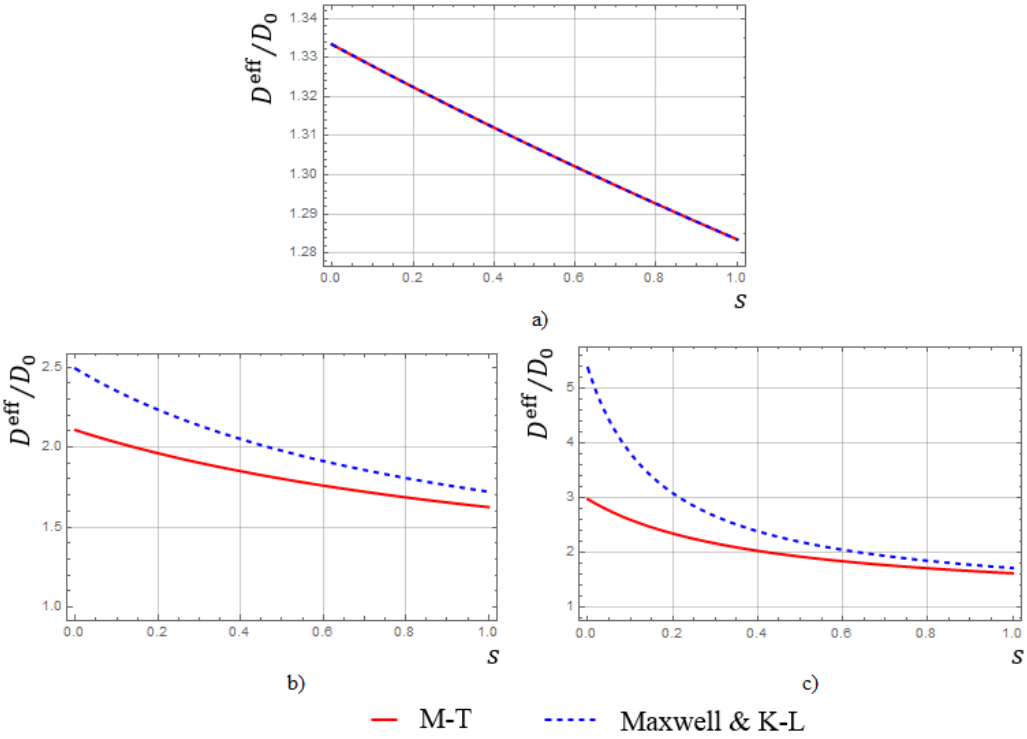


**Fig. 2.** Dependencies of the effective diffusion coefficient on the segregation factor for material with spherical pores (a), randomly oriented oblate pores (b), and randomly oriented prolate pores (c)

A comparison of dependencies of the diffusion coefficient on the segregation factor for material with pores that have certain preferential orientation accompanied by random scatter ($\lambda$ = 3) is shown in Fig. 3. The three shapes of the prohibition zone in Kanaun-Levin discussed in section 3 are considered.

Again, decreasing the segregation factor increases the difference between models. The segregation is seen to have a greater influence on the results obtained within the Maxwell homogenization scheme. Kanaun-Levin scheme is close to the Mori-Tanaka scheme in the case when the shape of the prohibition zone coincides with the shape of individual inhomogeneity. Note that introduction of the spherical prohibition zone in the Kanaun-Levin scheme for material with prolate spheroidal pores yields physically incorrect results at low

values of the segregation factor, since in this case, $\phi = 0.1$ is close to the "mathematical limit" discussed in the previous section.

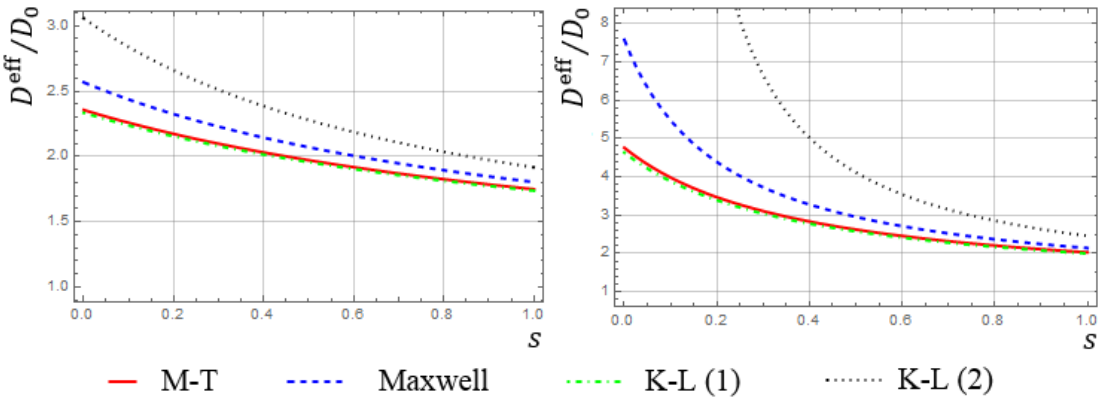


**Fig. 3.** Dependencies of the effective diffusion coefficient on the segregation factor for material with oblate pores ($D_{11}^{\text{eff}}$, left) and prolate pores ($D_{33}^{\text{eff}}$, right) that have certain preferential orientation accompanied by random scatter ($\lambda = 3$)

Since the volume fraction cannot take all values from 0 to 1 in the cases of Kanaun-Levin and Maxwell homogenization methods due to the "mathematical limit", let us investigate the dependencies of the effective diffusion coefficient on the volume fraction of pores calculated on the base of Mori-Tanaka scheme. Figure 4 compares the effective diffusivity at various orientational scatters at $s = 0.5$. At low concentrations, the oblate spheroidal pores affect diffusivity within the plane of isotropy more than diffusivity along the axis of symmetry (the last one is close to $D_0$). The situation is the opposite in the case of prolate spheroids. For the sake of brevity, we do not provide dependencies corresponding to the microstructures that have a lower influence on the overall diffusivity.

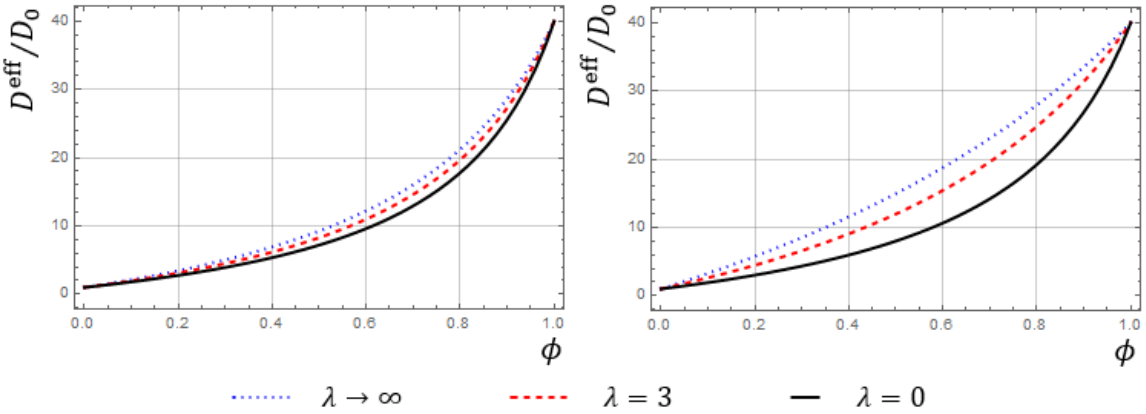


**Fig. 4.** Dependencies of the effective diffusion coefficient on the volume fraction of oblate pores ($D_{11}^{\text{eff}}$, left) and prolate pores ($D_{33}^{\text{eff}}$, right) at different values of the scatter parameter; $s = 0.5$

According to Fig. 4, left, orientational scatter does not affect significantly the overall diffusivity in the plane of isotropy in the case of oblate spheroidal pores. Thus, the orientational scatter identifies the direction of the maximum effective diffusivity, whereas the effective properties in this direction can be calculated on the basis of formulas for isotropic material. In the case of prolate spheroidal pores (Fig. 4, right), the orientation scatter plays a more significant role. It must be accounted for in estimations of the overall diffusivity. Also,

the comparison of black lines in Fig. 4 allows concluding that in the case of isotropic material, consideration of oblate spheroidal pores with $\gamma = 0.1$ is equivalent to consideration of prolate spheroidal pores with $\gamma = 10$.

In this section, it is shown that the presence of pores can increase the diffusion coefficient. In some cases, even a slight increase in concentration can change the material behavior, so quantitative characteristics of the mass transport process must be accounted for in diffusion problems. In particular, an increase in the diffusion coefficient by several times can be important in problems related to hydrogen degradation of metals. Hydrogen is known to have a big influence on the physical properties of the host material even at small concentrations. It is believed that hydrogen diffuses through metals lattice and leads to cracking along grain boundaries that, in turn, change the overall concentration directly during the mass transport process, since hydrogen can be trapped inside the new microcracks [5,6,34,35]. The results of the present paper can be used in modeling this process.

## 5. Conclusion

The paper calculates the effective diffusion coefficients of transversely isotropic material. The overall anisotropy is assumed to be induced by the shape and preferential orientation of spheroidal inhomogeneities, whereas the host matrix is assumed to be isotropic. The focus is on the segregation effect that is the main difference between diffusivity and conductivity problems. Mori-Tanaka, Kanaun-Levin, Maxwell general, and Maxwell linearized homogenization methods are used. Wiener's and Hashin-Shtrikman's bounds are modified to account for the segregation effect in the diffusivity problem. The effective properties calculated by means of various homogenization methods are checked to satisfy the modified bounds.

It is shown that accounting for the constant jump in concentration at the matrix/inhomogeneity interface increases the effective diffusivity. In the cases of non-spherical pores, such an increase may change the result significantly. In general, the segregation effect is more pronounced when applying Maxwell and Kanaun-Levin homogenization schemes that introduce some kind of effective inhomogeneity. Introduction of the segregation factor smaller than one increases the difference in the results obtained within Mori-Tanaka, Maxwell, and Kanaun-Levin methods.

The presented methodology of determining the effective diffusivity accounting for the segregation effect can be directly extended to orthotropic materials with isotropic matrix and overall anisotropy induced by inhomogeneities. To this end, one should consider ellipsoidal inhomogeneities instead of spheroidal ones. An extension to the case of ellipsoidal inhomogeneities arbitrarily oriented in an anisotropic matrix also can be made following [20] for conductivity.

## References

[1] Mishin YM. 50 years of grain boundary diffusion: what do we know about it today? *Defect and Diffusion Forum.* 2001;194: 1113-1126.

[2] Gordillo JA. Effective Diffusion Coefficient. *Defect and Diffusion Forum.* 2018;384: 130-135.

[3] Gerasimov RM, Volegov PS., Gribov DS. Modeling of microcracks and edge dislocations trapping of impurity atoms in Fe-C: MD simulation. *AIP Conference Proceedings.* 2021;2371(1): 020003.

[4] Mehrer H. *Diffusion in solids: fundamentals, methods, materials, diffusion-controlled processes.* Springer; 2007.

[5] [Nair SV, Jensen RR, Tien JK. Kinetic enrichment of hydrogen at interfaces and voids by dislocation sweep-in of hydrogen. *Metallurgical Transactions A.* 1983;14(2): 385-393.

[6] Pressouyre GM. A classification of hydrogen traps in steel. *Metallurgical Transactions A.* 1979;10(10): 1571-1573.
[7] Hart EW. Thermal conductivity. *Acta Metallurgica.* 1957;5: 597-605.
[8] Barrer RM. Diffusion and permeation in heterogeneous media. *Diffusion in Polymers.* 1968: 165-217.
[9] Zhang Y, Liu L. On diffusion in heterogeneous media. *American Journal of Science.* 2012;312(9): 1028-1047.
[10] Kaur I, Mishin Y, Gust W. *Fundamentals of Grain and Interphase Boundary Diffusion.* Wiley; 1995.
[11] Umbanhowar PB, Lueptow RM, Ottino JM. Modeling segregation in granular flows. *Annual Review of Chemical and Biomolecular Engineering.* 2019;10: 129-153.
[12] Belova IV, Murch GE. Diffusion in nanocrystalline materials. *Journal of Physics and Chemistry of Solids.* 2003;64(5): 873-878.
[13] Belova IV, Murch GE. The effective diffusivity in polycrystalline material in the presence of interphase boundaries. *Philosophical magazine.* 2004;84(1): 17-28.
[14] Knyazeva AG, Grabovetskaya GP, Mishin IP, Sevostianov I. On the micromechanical modelling of the effective diffusion coefficient of a polycrystalline material. *Philosophical Magazine.* 2015;95(19): 2046-2066.
[15] Giraud A, Sevostianov I, Kushch VI, Cosenza P, Prêt D, Barthélémy JF, Trofimov A. Effective electrical conductivity of transversely isotropic rocks with arbitrarily oriented ellipsoidal inclusions. *Mechanics of Materials.* 2019;133: 174-192.
[16] Łydżba D, Różański A, Sevostianov I, Stefaniuk D. Principle of equivalent microstructure in micromechanics and its connection with the replacement relations. Thermal conductivity problem. *International Journal of Engineering Science.* 2019;144: 103126.
[17] Vilchevskaya E, Sevostianov I. Effect of pore shapes on the overall electrical conductivity of cathode material in Li-ion batteries. *International Journal of Engineering Science.* 2020;146: 103187.
[18] Frolova KP, Vilchevskaya EN. Effective diffusion coefficient of a porous material applied to the problem of hydrogen damage. In: Polyansky VA, Belyaev AK. (eds.) *Advances in Hydrogen Embrittlement Study.* Springer; 2021. p.113-130.
[19] Sevostianov I, Levin V, Radi E. Effective properties of linear viscoelastic microcracked materials: Application of Maxwell homogenization scheme. *Mechanics of Materials.* 2015;84: 28-43.
[20] Kachanov M, Sevostianov I. Micromechanics of materials, with applications. In: *Solid Mechanics and Its Applications.* Cham: Springer; 2018. p.249.
[21] Kachanov M, Sevostianov I. On quantitative characterization of microstructures and effective properties. *International Journal of Solids and Structures.* 2005;42(2): 309-336.
[22] Kalnin JR, Kotomin EA, Maier J. Calculations of the effective diffusion coefficient for inhomogeneous media. *Journal of physics and chemistry of solids.* 2002;63(3): 449-456.
[23] Fricke H. A mathematical treatment of the electric conductivity and capacity of disperse systems I. The electric conductivity of a suspension of homogeneous spheroids. *Physical Review.* 1924;24(5): 575.
[24] Markov KZ. Elementary micromechanics of heterogeneous media. In: Markov K, Preziosi L. (eds.) *Heterogeneous Media. Modeling and Simulation in Science, Engineering and Technology.* Boston, MA: Birkhäuser; 2000. p.1-162
[25] Mossotti OF. *Sur les forces qui régissent la constitution intérieure des corps: aperçu pour servir à la détermination de la cause et des lois de l'action moléculaire.* De l'Imprimerie royale; 1836.
[26] Mori T, Tanaka K. Average stress in matrix and average elastic energy of materials with misfitting inclusions. *Acta metallurgica.* 1973;21(5): 571-574.

[27] Benveniste Y. On the Mori-Tanaka's method in cracked bodies. *Mechanics Research Communications.* 1986;13(4): 193-201.
[28] Maxwell JC. *A treatise on electricity and magnetism.* Clarendon press; 1873.
[29] Sevostianov I. On the shape of effective inclusion in the Maxwell homogenization scheme for anisotropic elastic composites. *Mechanics of Materials.* 2014;75: 45-59.
[30] Sevostianov I, Giraud A. Generalization of Maxwell homogenization scheme for elastic material containing inhomogeneities of diverse shape. *International Journal of Engineering Science.* 2013;64: 23-36.
[31] Sevostianov I, Kachanov M. Elastic fields generated by inhomogeneities: Far-field asymptotics, its shape dependence and relation to the effective elastic properties. *International Journal of Solids and Structures.* 2011;48(16-17): 2340-2348.
[32] Kanaun SK. Approximation of a self-consistent field for the elastic composite medium. *Journal Applied Mechanics and Technic Physics.* 1977;2: 166-169.
[33] Levin VM. Determination of elastic and thermoelastic constants of composite materials. *Akademiia Nauk SSSR, Izvestiia, Mekhanika Tverdogo Tela.* 1976: 137-145. (In Russian)
[34. Koyama M, Akiyama E, Tsuzaki K. Hydrogen-induced delayed fracture of a Fe–22Mn–0.6 C steel pre-strained at different strain rates. *Scripta Materialia.* 2012;66(11): 947-950.
[35] Luo H, Zhao B, Pan Z, Fu Y, Li X. Hydrogen induced microstructure evolution and cracking mechanism in a metastable dual-phase high-entropy alloy. *Materials Science and Engineering: A.* 2021; 141490.

## THE AUTHORS

**Frolova K.P.**
e-mail: kspfrolova@gmail.com
ORCID: 0000-0003-0376-4463

**Vilchevskaya E.N.**
e-mail: vilchevska@gmail.com
ORCID: 000-0002-5173-3218